European Review for Medical and Pharmacological Sciences 2021; 25: 2949-2957

7q35q36.3 deletion and concomitant 20q13.2q13.33 duplication in a newborn: *familiar case*

D. DELL'EDERA[1], A. ALLEGRETTI[1], F. FORTE[2], R.A. DELL'EDERA[3], M.T. DELL'EDERA[3], A.A. EPIFANIA[1], L. MERCURI[4], C.R. CATACCHIO[4], A. MITIDIERI[1], F. SIMONE[1], M. VENTURA[4]

[1]Unit of Medical Genetics, "Madonna delle Grazie" Hospital, Matera, Italy
[2]Pediatric Unit, "Madonna delle Grazie" Hospital, Matera, Italy
[3]Universitatea de Vest Vasile Goldis din Arad Facultatea de Medicină: Universitatea de Vest Vasile Goldis din Arad Facultatea de Medicina, Arad, Romania
[4]Department of Biology, University "Aldo Moro", Bari, Italy

Abstract. – OBJECTIVE: Array-CGH is a powerful tool in identifying and characterizing complex genomic rearrangements smaller than 5-10 megabase (Mb), for which classical cytogenetic approaches are not sensitive enough. The use of Array-CGH has increased of 10-20% the detection rate of unbalanced cryptic rearrangements, such as deletions and/or duplications.

PATIENTS AND METHODS: We present here the first report of a patient with 7q35q36.3 microdeletion and concomitant 20q13.2q13.33 microduplication detected by array-CGH and confirmed by reiterative FISH experiments associated with dysmorphism, development delay, Long QT syndrome (LQTS), complex congenital heart disease, pulmonary hypertension, hypotonia, respiratory distress, cognitive deficit.

RESULTS: We proved that this unbalanced rearrangement was due to an adjacent-1 segregation that occurred in the mother, carrier of a balanced translocation between chromosomes 7 and 20. The same unbalanced rearrangements were also found in the proband's maternal uncle, who had been given a clinical diagnosis of Dandy-Walker/Rubinstein-Taybi syndromes in the past. Given the above-mentioned observations, the proband's uncle is not affected by Dandy-Walker/Rubinstein-Taybi syndromes, but by a genomic syndrome highlighted by array-CGH.

CONCLUSIONS: The Array-CGH allowed us to understand that the loss of several genes is expressed with clinical manifestations due to the concomitance of several syndromes, each related to the malfunction of a "specific disease gene". For these reasons, the genotype-phenotype correlation in these cases is more complex. This study confirms that the array-CGH is useful in identifying pathologies that were considered idiopathic until a few years ago.

Key Words:
7q microdeletion, 20q microduplication, Array comparative genomic hybridization (array-CGH), Bacterial artificial chromosome (BAC), Reciprocal translocation, Long QT syndrome.

Introduction

Reciprocal translocations are commonly balanced exchanges between non-homologous chromosomes usually associated with normal phenotype.

Heterozygous carriers of translocations can induce abnormal meiosis, thus resulting in an increased rate of miscarriage[1]. The pregnancy loss is related to meiotic segregation since meiosis in translocation heterozygotes may generate gametes harboring unbalanced rearrangements, such as duplications and deletions.

Unbalanced chromosomal rearrangements can be studied by array comparative genomic hybridization (array-CGH) that is able to identify at high resolution (5-10 Mb) the genetic causes of complex phenotypes, usually only partially detectable (9.5%) by classical cytogenetics[2-5]. When the array-CGH was not discovered, these genomic alterations were called "idiopathic syndromes".

Compared to fluorescence *in situ* hybridization (FISH), array-CGH is a faster technique in detecting in a single experiment unbalanced chromosomal rearrangements without *a priori* knowledge. On the other hand, array-CGH has a relevant limitation in detecting balanced rear-

Corresponding Author: Domenico Dell'Edera, MD; e-mail: domenicodelledera68@gmail.com

rangements where, instead, classical and molecular cytogenetics (FISH) are still used as elective strategies.

Here, we present the first report of a patient with 7q35q36.3 microdeletion and 20q13.2q13.33 microduplication detected by array-CGH and deeply studied by reiterative FISH experiments, and associated with dysmorphism, development delay, Long QT syndrome (LQTS), complex congenital heart disease, pulmonary hypertension, hypotonia, respiratory distress, and cognitive deficit. The unbalanced rearrangements resulted as products of an adjacent 1 segregation of a balanced translocation (7q;20q) carried by the mother of the patient. The same unbalanced rearrangements were also found in the proband's maternal uncle.

Clinical Report

The subject of this study is a six-month-old girl (D.A.) (Figure 1: family tree III4). Her mother (L.M.) (Figure 1: family tree II2) reported four pregnancies: two of them terminated during the first trimester as spontaneous miscarriages (Figure 1: family tree III1 and III2), one birth resulted in D.F. (Figure 1: family tree III3) and the fourth pregnancy resulted in D.A (Figure 1: index case, family tree III4). In addition, L.M. reported to have a 27-year-old brother, L.F. (Figure 1: family tree II3), who at the age of ten, was diagnosed with suspicion of Dandy-Walker malformation-Rubinstein Taybi syndrome by two

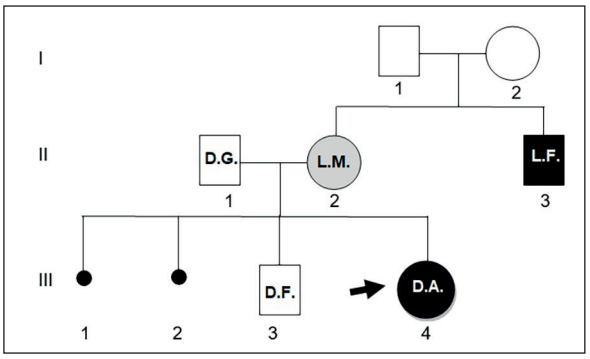

Figure 1. (Pedigree). II1: father of D.A.; II2: mother of D.A.; III1 and III2: two miscarriages in the first trimester of pregnancy; III3: brother of D.A.; III4: D.A. (case index); II3: uncle of D.A. **Black** (II3 and III4): patient with 7q35q36.3 deletion and 20q13.2q13.33 duplication detected by array-CGH. **Grey** (II2): FISH analyses revealed that the mother (II2) was carrier of a balanced translocation between the q terminal arm of chromosome 7 and the q terminal arm of chromosome 20. **White** (II1 and III3): normal male karyotype. our analyzed individuals.

different groups of clinicians. These syndromes have never been confirmed through the use of biomolecular investigations.

The only certain clinical signs we have been able to know about Mr. L.F. are: rotation of the cerebellar vermis, visible by magnetic resonance; dilation of the fourth ventricle; cardiac anomalies, and intellectual disabilities.

L.M. prenatal history showed no evidence of teratogen exposure or any other relevant exposures or pathologies. Ultrasound reports during weeks 14 and 25 of gestation showed no morphological alterations.

The delivery of D.A. was natural, and the baby was born at term (39 weeks and six days) with a weight of 2230 grams. She showed APGAR indices of six, seven and eight at one, five and ten minutes after birth, respectively. D.A. was transferred to the Neonatal Intensive Care Unit (NICU) due to the low weight (inferior 2500 grams) and the presence of dysmorphic elements (microcephaly, cup-shaped ears, hypotelorism, squat and short neck, clenched hands with overlapping fingers, active and passive hypertonus of the limbs, absent cry, posture with extended lower limbs and tense and abducted upper limbs). Furthermore, she showed tense and not very palpable abdomen, the heart rate at 140 beats/minute, respiratory rate at 45 acts/minute and blood pressure at 53/43 mmHg.

Blood tests showed an increase in aspartate aminotransferase (AST: 537 IU/L) and alanine aminotransferase (ALT: 247 IU/L), leukocytes (36970 cells/uL), serum creatinine (1.8 mg/dL), Reactive Protein C (8,9 mg/dL), creatine kinase (CK or CPK: 217 IU/L), creatine kinase MB (CK-MB: 42.9 IU/L) and a decrease in sodium levels (125 mmol/L). In addition, the newborn girl had been subjected to antibiotic therapy due to *Escherichia coli* detection on blood culture and pharyngeal swab.

Upon entering UTIN, continuous monitoring of tissue oxygenation (kidney and brain) was performed through Near-Infrared Spectroscopy (NIRS), while brain electrical activity was assessed through the use of Cerebral Function Monitoring (CFM). Given the difficulty in breathing highlighted since birth, the Nasal Continuous Positive Airway Pressure (nCPAP) was applied to the D.A. Echocardiography showed: situs solitus, levocardia; atrial septal defect (DIA) near the superior vena cava (high caval), moderate tricuspid insufficiency which indicates a high blood pressure (PAPs about 80 mmHg); normal-sized left

heart chambers; preserved biventricular kinesis; pulmonary artery of normal caliber and with normoconfluent branches; patent ductus arteriosus with a moderate bidirectional shunt; aortic arch and aortic isthmus of normal caliber and flowmetry; normopulsing abdominal aorta; absence of pericardial effusion. To treat pulmonary hypertension, the following therapy has been implemented: dobutamine and milrinone with continuous infusion.

Given the persistence of high lung pressure associated with an unconvincing radiographic picture, on the seventh day of her life, D.A. was intubated and treatment with High Frequency Oscillation (HFO) with nitric oxide was started. At the following echocardiographic control there was a sharp drop in lung resistance (right ventricle pressure: 25 mmHg) and the presence of two apical muscular ventricular septal defect (VSD) was assessed. The nitric oxide dosage was reduced and suspended after about 24 hours, followed by a milrinone suspension after a few days. On this occasion, a bronchoalveolar lavage was performed which resulted negative for *Clamidya*, *Ureoplasma*, and *Mycoplasma*.

On the tenth day of D.A.'s life, an electrocardiogram (ECG) was performed detecting the presence of a QTc (QT corrected according to the frequency) lengthened by 480 msec in V5 (normal values: 350-440 msec). For this reason, D.A. started therapy with propanolol hydrochloride (beta blocker) initially at a dosage of 1 mg/kg/die, and then, reached a dose of 7 mg/kg/die in three administrations for the persistence of the extended QTc (values between 440 and 490 msec). In addition, the ECG detected the presence of ventricular pre-excitation (a delta wave at the beginning of the QRS complex).

The abdominal ultrasound showed:
- Liver dimensions within the limits of normality without appreciable eco structural alterations;
- Gallbladder with endoluminal biliary sludge and moderate concentric thickening of the wall;
- Mild intrahepatic biliary duct dilatation;
- Pancreas not explorable;
- Spleen within normal limits;
- Kidneys size within the limits with regular eco-structure.

The magnetic resonance imaging (MRI) of the brain showed brachycephaly, a corpus callosum thin and incomplete, with reduced thickness of the splenium and not recognizable rostrum, a moderately squared aspect of the posterior sectors of the lateral ventricles, mild cerebellar vermis hypoplasia and mega cisterna magna, no significant signal alterations of the nerve tissue, regular progression of myelination. Substantially regular the volume of the ventricular system. The regular amplitude of the pericerebral spaces. Neonatal screenings for phenylketonuria, hypothyroidism, and cystic fibrosis were negative.

The girl, after two months of hospitalization, was discharged with suitable therapy. Physical examination at release revealed a weight of 3240 grams, pink color, good state of hydration, regular cardiorespiratory fitness, abdomen treatable, moderate hypertonus of the four limbs. The discharge summary was:
- Newborn with dysmorphism;
- Development delay;
- LQTS syndrome (LQTS);
- Complex congenital heart disease;
- Pulmonary hypertension;
- Hypotonia;
- Respiratory distress;
- Cognitive deficit.

To evaluate genomic alterations' possible presence, genomic analysis was carried out using array-CGH, karyotype and molecular cytogenetics.

Methods

Array-CGH

Cytogenetic and array-CGH analyses were performed on the peripheral blood of the patient, her parents, and her brother. High-resolution chromosomes were QFQ banded using the standard procedure[6]. Genomic DNA was extracted from peripheral blood leukocytes using "QIAamp® DSP DNA Blood Mini" commercial kit from Qiagen (DNA IQTM System-Qiagen S.r.l., Milan, Italy), in accordance with the manufacturer's specifications. The array-CGH analysis was performed using ISCA V.2, 4x180K oligo platforms (Oxford Gene Technology, Begbroke Science & Business Park, Begbroke Hill, Begbroke OX5 1PF, UK), with 25 Kb probe spacing (higher resolution in ISCA region). Experiments were conducted according to the manufacturer's protocol. Male and female commercial reference DNAs, provided by Promega G 1521 (Madison, WI, USA), were used for the analysis. The slides were scanned with Innoscan 710 Microarray Scanner; captured

Table I. BAC clones labelled with specific fluorophores, their genomic position on GRCh37 human release and the followed strategies.

BAC clone	Fluorescent dye	Mapping (GRCh37/hg19)	Strategy
RP11-648P19	CY3	chr7:151,029,463-151,180,365	Probe mapping into the deleted region
RP11-959A2	FITC	chr20:55,845,790-56,022,780	Probe mapping into the duplicated region
RP11-696D4	CY5	chr7:62,003,599-62,160,915	Probe mapping downstream with respect to the centromere in order to identify chr7

images were analyzed with CytoSure Interpret Software version 4.10. Genomic region analysis was performed according to the human reference sequence hg 19 Genome Reference Consortium (GRCh 37). The copy number variations (CNVs) founded in the proband were compared with genomic variants present on different databases [DECIPHER: https://decipher.sanger.ac.uk, UCSC Genome Browser: https://genome.ucsc.edu, Clinical Genome Resource (Clingen): http://clinicalgenome.org; Troina Database of Human CNVs: http://gvarianti.ho- melinux.net/gvariantib37/index.php].

Cytogenetic Analysis With FISH

The array-CGH results were confirmed by fluorescence *in situ* hybridization (FISH). Metaphase spreads of each investigated individual were obtained from phytohaemagglutinin (PHA)-stimulated whole blood cultures. FISH experiments were performed using human bacterial artificial chromosome (BAC) clones (Table I) directly labeled by nick-translation with Cy3-dUTP (Perkin-Elmer, Waltham, MA, USA), Cy5-dUTP (Perkin-Elmer) and fluorescein-dUTP (Enzo Life Sciences, Farmingdale, NY, USA) as described by Bentz[7], with minor modifications. Briefly, 300 ng of labeled probe were used for the FISH experiments; hybridization was performed at 37°C in 2 x SSC, 50% (v/v) formamide, 10% (w/v) dextran sulphate and 3 µg sonicated salmon sperm DNA, in a volume of 10 µL. Post hybridization washing was at high stringency (60°C in 0.1 x SSC, three times). Fluorescence signal intensity from DAPI, Cy3, Cy5 and fluorescein was detected with specific filters using a Leica DMRXA2 epifluorescence microscope (Leica Microsystems GmbH, Wetzlar, Hesse, Germany) equipped with a cooled C.C.D. camera. Digital images were separately recorded as grayscale pictures and subsequently pseudocolored and merged using Adobe Photoshop software (Adobe, San Jose, CA, USA).

Results

Array-CGH performed on D.A. detected a microdeletion on the long arm of chromosome 7 (7q35q36.3 = 12.55 Mb) and a microduplication on the long arm of chromosome 20 (20q13.2q13.33 = 10.28 Mb) (Figures 2 and 3).

The chromosomal region 7q35q36.3 (chr7: 146,581,463-159,128,155) contains the OMIM "Morbid" genes ASB10, CDK5, CNTNAP2, DNAJB6, DPP6, EZH2, KCNH2, KMT2C, LMBR1, MNX1, NCAPG2, NOS3, PRKAG60 and XHCC2DR (Table II).

The chromosomal region 20q13.2q13.33 (chr20: 52,667,758-62,949,155) harbors the fol-

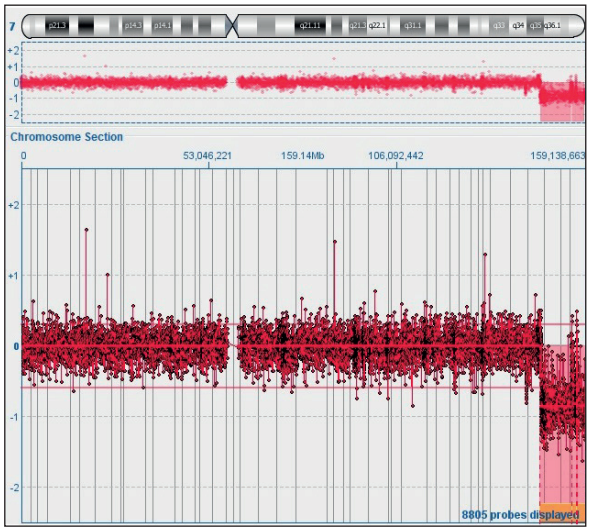

Figure 2. Microdeletion on the long arm of chromosome 7 (7q35q36.3) found in D.A. and L.F.. The chromosomal region 7q35q36.3 contains the OMIM "Morbid" genes *ASB10*, *CDK5*, *CNTNAP2*, *DNAJB6*, *DPP6*, *EZH2*, *KCNH2*, *KMT2C*, *LMBR1*, *MNX1*, *NCAPG2*, *NOS3*, *PRKAG60* and *XHCC2DR*. The top panel shows the ideogram of chromosome 7 with the 7q35q36.3 microdeleted region marked in a small red box (chr7: 146,581,463-159,128,155). The scatter plot of the CGH-array data, in the central panel, shows a ~12.55 Mb microdeletion on chromosome arm 7q found in D.A. and L.F.

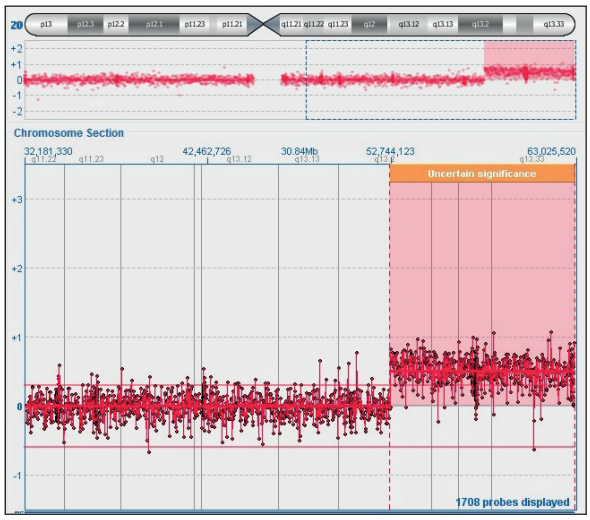

Figure 3. Array-CGH performed on D.A. and L.F. detected a microduplication on the long arm of chromosome 20 (20q13.2q13.33= ~10,28 Mb). The chromosomal region 20q13.2q13.33 harbors the following OMIM "Morbid" genes *ATP5E*, *AURKA*, *CHRNA4*, *COL9A3*, *CYP24A1*, *DNAJC5*, *EDN3*, *EEF1A2*, *GATA5*, *OS*, *KCRNQ2*, *MC3*, *PCK1*, *PRPF6*, *RTEL1*, *SLC17A9*, *SOX18*, *STX16*, *TUBB1*, *VAPB*. The top panel shows the ideogram of chromosome 20 with the 20q13.2q13.33 microduplicated region marked in a small red box (chr20: 52,667,758-62,949,155). The scatter plot of the array-CGH data, in the central panel, shows a ~10,28 Mb microduplication of 20q13.2q13.33 region found in D.A. and L.F.

lowing OMIM "Morbid" genes ATP5E, AURKA, CHRNA4, COL9A3, CYP24A1, DNAJC5, EDN3, EEF1A2, GATA5, OS, KCRNQ2, MC3, PCK1, PRPF6, RTEL1, SLC17A9, SOX18, STX16, TUBB1, VAPB (Table II). Array-CGH of the parents was found to be normal.

Furthermore, the maternal uncle of D.A. (L.F. in Figure 1) presented a clinical picture associated with Dandy-Walker/Rubinstein Taybi syndrome.

To understand if there was a connection between what was found in D.A. and her uncle, we have extended the array-CGH analysis to L.F.

Array-CGH performed on L.F. found the same genomic structure found in D.A.: del7q35q36.3 (chr7: 146,581,463-159,128,155) and dup20q13.2q13.33 (chr20: 52,667,758-62,949,155).

To establish if what was highlighted was the result of a familial balanced reciprocal translocation, we performed peripheral blood karyotype followed by FISH on both the mother of D.A. (LM, family tree II2 – ID43/19) and her brother (L.F., family tree II3 – ID 42/19).

In silico analysis of the candidate regions using UCSC genome browser allowed us to choose three BAC clones as FISH probes (Table I) to detect the supposed translocation.

FISH analyses revealed that the mother (Figure 4B, ID 43/19) was carrier of a balanced translocation between the terminal region of long arm (q) of chromosome 7 and the terminal region of long arm (q) of chromosome 20. Thus, the array-CGH negative result was due to balanced translocation. The FISH results of the uncle (Figure 4A, ID 42/19) showed the deletion of the terminal region of long arm (q) of chromosome 7 and the duplication of the terminal region of long arm (q) of chromosome 20.

To define the breakpoints of the rearrangements, FISH experiments were performed on metaphases from the uncle (Figure 1: family tree II3, L.F.). *In silico* analysis of the candidate regions using UCSC genome browser allowed us to choose two BAC clones (RP11-702N14 and RP11-368H3) as probes for FISH experiments (Figure 5). The results showed a normal chromosome 7 with a red signal, a derivative chromosome 7 identified by the presence of both the red and green signals at lower intensity due to the split of the clones overlapping the breakpoints, and two normal chromosomes 20 with green signals (Figure 5).

Table II. The 34 affected genes contained in the altered regions on chromosomes 7 and 20, as annotated on the RefSeq database.

Rearrangement	Chromosome	Start (hg19)	End (hg19)	Genes Involved (OMIM "Morbid")
7q35q36.3del	chr7	146,581,463	159,128,155	ASB10, CDK5, CNTNAP2, DNAJB6, DPP6, EZH2, KCNH2, LMBR1, MNX1, NOS3, PRKAG2, SHH, WDR60, XRCC2, KMT2C, NCAPG2.
20q13.2q13.33dupl	chr20	52,667,758	62,949,155	ATP5E, AURKA, CHRNA4, COL9A3, CYP24A1, DNAJC5, EDN3, EEF1A2, GNAS, KCNQ2, MC3R, OSBPL2, PCK1, PRPF6, RTEL1, SLC17A9, SOX18, STX16, TUBB1, VAPB, GATA5.

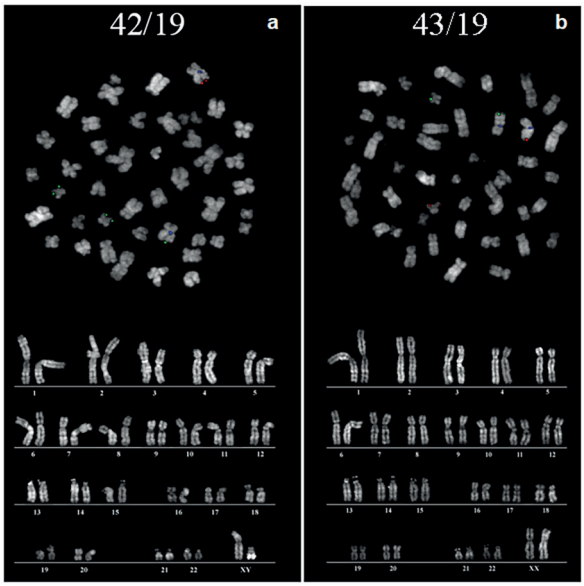

Figure 4. Cohybridization of RP11-648P19 (red), RP11-959A2 (green) and RP11-696D4 (blue) on **a.** 42/19 shows the 7q deletion (single red signal, on the normal chromosome 7) and the 20q duplication (triple green signals, two on the normal chromosome 20 and one on the derivative chromosome 7) and **b.** on 43/19 shows the translocation between chr7 and chr20 (chr t7 with blue and green signals, chr t20 with red signal). Lower lines both karyotypes are reported.

The FISH results of the uncle (Figure 6: ID 42/19) showed the deletion of the long arm (q) of chromosome 7 and the duplication of the long arm (q) of chromosome 20. FISH experiments were also performed on D.F. (Figure 6: ID 129/20) and on a cousin (Figure 6: ID 145/20) of Mrs. L.M., both phenotypically normal and with no signs of pathologies. Cousin (Figure 6: ID 145/20) told us that he had two previous pregnancies, both ended by miscarriage in the first trimester of pregnancy. FISH analyses showed normal chromosomes 7 and 20. All the results are summarized in Figure 6.

A deep study of the gene content of the unbalanced genomic regions detected 16 deleted and 21 duplicated genes on chromosome 7 and 20, respectively (Table II).

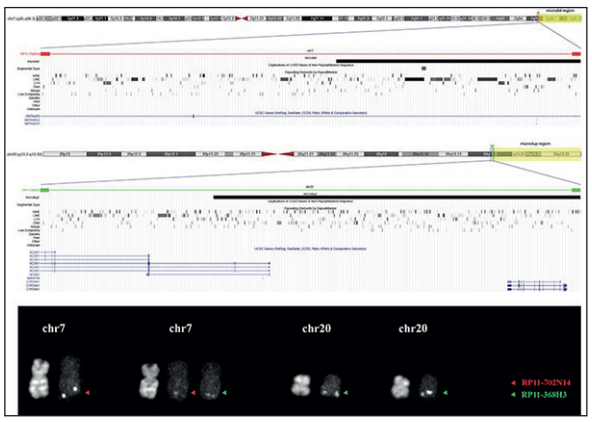

Figure 5. Above: ideogram of chr7 with a highlight of the deleted region and a zoom in the region of the proximal breakpoint. In red the BAC clone RP11-702N14 used to define the breakpoint; ideogram of chr20 with a highlight of the duplicated region and a zoom in the region of the proximal breakpoint. In green the BAC clone RP11-368H3 used to define the breakpoint. Below: FISH results are reported (see the text).

Discussion

Translocations are balanced rearrangements that in heterozygotes can cause meiotic missegregation, thus obtaining unbalanced gametes. We here documented and studied an unbalanced re-

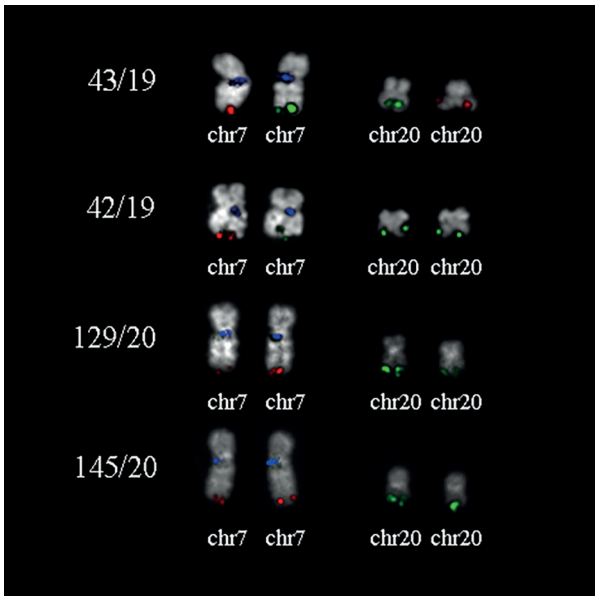

Figure 6. Cohybridization of RP11-648P19 (red), RP11-959A2 (*green*) and RP11-696D4 (blue) on extracted metaphase chromosomes in the four analyzed individuals. FISH analyses revealed that the mother (ID 43/19, family tree II2) was carrier of a balanced translocation between the q terminal arm of chromosome 7 and the q terminal arm of chromosome 20. The FISH results of the uncle (ID 42/19, family tree III4) showed the deletion of the q terminal region of chromosome 7 and the duplication of the q terminal region of chromosome 20. FISH experiment was also performed on the D.F. (III3 of the family tree, ID 129/20) and on a cousin (ID 145/20) of Mrs. L.M., both phenotypically normal and with no signs of pathologies. FISH analyzes, chromosomes 7 and 20 appear normal.

arrangement due to missegregation of a balanced translocation 7q;20q likely occurred in one of the grandparents of maternal lineage (Figure 1: I1 or I2 of the family tree).

Microdeletions and/or microduplications lead to the loss of functions of several genes; as a consequence, there is the manifestation of a complex phenotype with the malfunctioning of several organs (multisystem diseases). We reported a 7q35q36.3 microdeletion (loss of 12.5 MB) resulting in the loss of a copy of 16 "Morbid" OMIM genes, including SHH, KCNH2, PRKAG2, and KMT2C.

KCNH2 gene is responsible for long QT syndrome type 2 (LQTS2) and encodes the α-subunits of the potassium channel protein I_{kr} [8], which is crucial for the repolarization of ventricular cardiomyocytes. According to the DECIPHER database, the haploinsufficiency index for KCNH2 is 8.86%, indicating that both point mutations and deletion events could lead to deleterious effect[9]. Three other patients harboring a deletion of the distal 7q region encompassing KCNH2 were found to have a LQTS2[10,11]. The previous literature suggests that in individuals with mutations in KCNH2 the use of chlorpheniramine, an H1 antihistamine, is strongly discouraged, as this drug blocks the functionality of the hERG channels, favoring the development of arrhythmogenic mechanisms[12].

PRKAG2 gene (Protein Kinase, AMP-Activated, non-catalytic subunit gamma-2) encodes an AMP-activated protein kinase (AMPK) activated by various cellular stresses that increase AMP levels and decrease ATP levels. Failure of the PRKAG2 gene is associated with Wolff-Parkinson-White syndrome (WPW). Diagnosis is often made based on the finding of heart rhythm disturbances. In our case, the index case exhibited a ventricular pre-excitation electrocardiogram (ECG) pattern (a delta wave at the beginning of the QRS complex), which is a typical expression of WPW syndrome[13].

SHH (Sonic Hedgehog) gene codes for a protein called "sonic hedgehog" which represents the best example of a morphogenetic molecule: this protein spreads producing a concentration gradient, and the cells of the embryo develop in different tissues, depending on the local concentration of SHH. In particular, the protein has a role of primary importance in the modelling of the ventral neuronal cell types along the entire central nervous system, the anterior-posterior axis during initiation of limb-bud outgrowth and the ventral somitic cells. An alteration of its function causes defects in the brain. At the MRI D.A. presents changes in the central nervous system (thin and incomplete corpus callosum, absence of the rostrum, cerebellar vermis hypoplasia) that are related to the inactivation of the SHH gene[14].

KMT2C gene encodes the enzyme histone-lysine N-methyltransferase 2C which, together with the histone-lysine N-methyltransferase D (KMT2D), forms the core of regulatory structures known as KMT2C/D COMPASS complexes. These proteins, interacting with other components of the COMPASS complex, modulate the activity of different cell types critical for embryonic morphogenesis and the development of the central nervous system. The loss of function of the KMT2C gene is responsible for type 2 Kleefstra syndrome (autosomal dominant)[15].

20q13.2q13.33 microduplication (10.28 Mb) led to the duplication of 21 OMIM "Morbid" genes, including GATA5, CHRNA4, and GNAS. GATA5 gene codes for a zinc finger transcriptional regulator with critical functions in embryonic differentiation and development. An alteration of its function causes autosomal dominant congenital heart defects (CHTD5)[16].

CHRNA4 (Cholinergic Receptor Nicotinic Alpha 4 Subunit) gene codes for a nicotinic acetylcholine receptor, which belongs to a superfamily of ionic binding channels that plays a role in rapid signal transmission to synapses. Mutations in this gene cause nocturnal frontal lobe epilepsy type 1 (ADNFLE). Alternative splicing produces multiple transcription variants[17].

GNAS (GNAS Complex Locus) gene is an imprinted complex locus that produces multiple transcripts through the use of alternative promoters and alternative splicing. In particular, the GNAS gene encodes the alpha subunit of a G protein. Gs-alpha subunit is biallelically expressed in almost all tissues and plays essential roles in a multitude of physiological processes. The G protein produced helps to stimulate the activity of adenylate cyclase. The latter is involved in the control of the production of different hormones that regulate the activity of the endocrine glands, such as the thyroid gland, pituitary gland, ovaries and testes (gonads), and adrenal glands. Other transcriptions produced by GNAS are expressed exclusively by the paternal or maternal allele. It also appears to be involved in McCune-Albright syndrome[18] and autosomal dominant progressive bone heteroplasia[19].

Many of the genes present in the regions 7q35q36.3 and 20q13.2q13.33 are involved in the correct neuropsychic development, and their alteration can be the basis of the neurological clinical picture present in the index case.

Array-CGH on D.A. (Figure 1) allowed us to re-evaluate her uncle's clinic picture (Figure 1, L.F): L.F. has the same genomic rearrangement found in D.A., which results from an unbalanced reciprocal translocation which led to a microdeletion of the short arm of chromosome 7 (q35q36.3 = 12.55 Mb) and a microduplication of the long arm of chromosome 20 (q13.2q13.33 = 10.28 Mb). Given the above-mentioned observations, the proband's uncle is not affected by Dandy-Walker/Rubinstein-Taybi syndromes, but by a genomic syndrome highlighted by array-CGH.

Conclusions

Array-CGH is useful in diagnosing subchromosomal aberrations. For this reason, its application is rapidly increasing. Furthermore, the array-CGH allows to precisely define the genomic region involved, and consequently, the "OMIM Morbid" genes contained. So, we can have an exact correlation between genotype and phenotype. Array-CGH allowed us to understand that the loss of several genes is expressed with clinical manifestations due to the concomitance of several syndromes, each related to the malfunction of a "specific disease gene". For these reasons, the genotype-phenotype correlation in these cases is more complex. This study confirms that the array-CGH is useful in identifying pathologies that until a few years ago were considered idiopathic. Actually, these pathologies are caused by submicroscopic chromosomal imbalances. Almost certainly, in the near future, more insights into the cause of some pathologies will be gained by the entry into clinical practice of Next Generation Sequencing (NGS) technologies.

Conflict of Interest

The Authors declare that they have no conflict of interests.

Acknowledgements

The authors wish to thank the "Association Gian Franco Lupo" ONLUS, "Association Anima Mundi" APS and "Association A.Ma.R.A.M." APS.

Statement of Ethics

Published research is comply with the guidelines for human studies and it's was conducted ethically in accordance with the World Medical Association Declaration of Helsinki. Authors declare under their own responsibility that the subjects studied have given their written consent to publish their case. The signed consent is kept in the Cytogenetic and Molecular Genetics unit.

Authors' Contribution

Mario Ventura, Arianna Allegretti and Domenico Dell'Edera made substantial contributions to conception and design. Fabio Forte, Ludovica Mercuri, Claudia Rita Catacchio, Angela Mitidieri, Rosalba Ardea Dell'Edera, Maria Teresa Dell'Edera, Francesca Simone and Annunziata Anna Epifania contributed to the acquisition, analysis and interpretation of data. Mario Ventura and Arianna Allegretti were involved in drafting the manuscript. Domenico Dell'Edera gave final approval of the version to be published. All authors read and approved the final manuscript.

References

1) Choi KH, You JS, Huh JW, Jeong YI, Kim MS, Jue MS, Park HJ. Fibro-osseous pseudotumor of the digit: a diagnostic pitfall of extraskeletal osteosarcoma. Ann Dermatol 2016; 28: 495-496.
2) Jacques C, Calleja LR, Baud'huin M, Quillard T, Heymann D, Lamoureux F, Ory B. miRNA-193a-5p repression of p73 controls cisplatin chemoresistance in primary bone tumors. Oncotarget 2016; 7: 54503-54514.
3) Xia YZ, Yang L, Xue GM, Zhang C, Guo C, Yang YW, Li SS, Zhang LY, Guo QL, Kong LY. Combining GRP78 suppression and MK2206-induced Akt inhibition decreases doxorubicin-induced P-glycoprotein expression and mitigates chemoresistance in human osteosarcoma. Oncotarget 2016; 7: 56371-56382.
4) Marina NM, Smeland S, Bielack SS, Bernstein M, Jovic G, Krailo MD, Hook JM, Arndt C, van den Berg H, Brennan B, Brichard B, Brown KL, Butterfass-Bahloul T, Calaminus G, Daldrup-Link HE. Comparison of MAPIE versus MAP in patients with a poor response to preoperative chemotherapy for newly diagnosed high-grade osteosarcoma (EURAMOS-1): an open-label, international, randomised controlled trial. Lancet Oncol 2016; 17: 1396-1408.
5) Ma K, Huang MY, Guo YX, Hu GQ. Matrine-induced autophagy counteracts cell apoptosis via the ERK signaling pathway in osteosarcoma cells. Oncol Lett 2016; 12: 1854-1860.
6) Setty BA, Jin Y, Houghton PJ, Yeager ND, Gross TG, Nelin LD. Hypoxic Proliferation of Osteosarcoma Cells Depends on Arginase II. Cell Physiol Biochem 2016; 39: 802-813.

7) Liu L, Qi XJ, Zhong ZK, Zhang EN. Nanomedicine-based combination of gambogic acid and retinoic acid chlorochalcone for enhanced anticancer efficacy in osteosarcoma. Biomed Pharmacother 2016; 83: 79-84.

8) Angelini A, Mavrogenis AF, Trovarelli G, Ferrari S, Picci P, Ruggieri P. Telangiectatic osteosarcoma: a review of 87 cases. J Cancer Res Clin Oncol 2016; 142: 2197-2207.

9) Li C, Guo D, Tang B, Zhang Y, Zhang K, Nie L. Notch1 is associated with the multidrug resistance of hypoxic osteosarcoma by regulating MRP1 gene expression. Neoplasma 2016; 63: 734-742.

10) Zheng X, Li X, Lyu Y, He Y, Wan W, Jiang X. Renal sympathetic denervation in rats ameliorates cardiac dysfunction and fibrosis post-myocardial infarction involving microRNAs. Med Sci Monit 2016; 22: 2751-2760.

11) Alizadeh S, Azizi SG, Soleimani M, Farshi Y, Kashani Khatib Z. The role of microRNAs in myeloproliferative neoplasia. Int J Hematol Oncol Stem Cell Res 2016; 10: 172-185.